

Absence of helical surface states in bulk semimetals with broken inversion symmetry

Carmine Ortix,¹ Jörn W. F. Venderbos,¹ Roland Hayn,² and Jeroen van den Brink¹

¹*Institute for Theoretical Solid State Physics, IFW Dresden, D01171 Dresden, Germany*

²*Aix-Marseille Université, CNRS, IM2NP-UMR 7334, 13397 Marseille Cedex 20, France*

(Received 10 July 2013; revised manuscript received 26 February 2014; published 14 March 2014)

Whereas the concept of topological band structures was developed originally for insulators with a bulk band gap, it has become increasingly clear that the prime consequences of a nontrivial topology—spin-momentum locking of surface states—can also be encountered in gapless systems. We show that point-group symmetries allow for *helical semimetals*, i.e., semimetals with Dirac-like topological surface states, to exist. The presence of this state, however, critically depends on the presence of crystal inversion symmetry. Using the paradigmatic example of mercury chalcogenides HgX ($X = \text{Te}, \text{Se}, \text{S}$), we show that an infinitesimally small broken inversion symmetry (BIS) renders the helical semimetallic state unstable. The BIS is also very important in the fully gapped topological insulating regime, renormalizing the surface Dirac cones in an anisotropic manner. As a consequence, the handedness of the Dirac cones can be flipped by a biaxial stress field.

DOI: [10.1103/PhysRevB.89.121408](https://doi.org/10.1103/PhysRevB.89.121408)

PACS number(s): 73.20.At, 71.55.Gs, 72.80.Sk

Introduction. The discovery of two- and three-dimensional (3D) topological insulators (TIs) [1–15] has brought to light a new state of quantum matter. This has had a tremendous impact in the field of fundamental condensed-matter physics as well as for potential applications in spintronics and quantum computation [16]. The TIs are insulating in the bulk but have topologically protected surface states [2,4,14] and the topology dictates that the metallic surface states are spin-momentum locked: surface electrons with opposite spin counterpropagate at the sample boundaries [3,4,7,9].

Materials with a TI band structure such as Sb [13], Bi_2Se_3 [17], and $\text{Bi}_{14}\text{Rh}_3\text{I}_9$ [15] often show the presence of a finite bulk carrier density. In such materials, the bulk Fermi surface *does not* simply swallow up the helical surface states. They survive and coexist with a bulk Fermi surface [13,18,19], leading to the notion of a *helical metal*. Similarly, in bulk semimetals with an inverted band ordering, surface Dirac-like states are expected to coexist with bulk metallic states [20,21], suggesting the presence of an analogous helical semimetallic state.

The lack of a full band gap in a semimetal makes the classification scheme in terms of a \mathbb{Z}_2 topological invariant meaningless, as it applies to insulators. Hence, the surface states of a semimetal are not protected by time-reversal symmetry alone. Here we show, however, that additional point-group symmetries can protect a surface Kramer’s doublet at the surface Brillouin-zone (BZ) center, the existence of which derives from the inverted bulk band ordering and defines the helical semimetallic state. The resulting “topological” surface states cannot be removed by adiabatic changes of the Hamiltonian preserving the nontrivial band ordering of the bulk electronic states unless the point-group symmetry protecting them is broken. Specifically, in this Rapid Communication, we will show that while a helical semimetallic state can be hosted in inverted semiconductors with full cubic symmetry (O_h), as in the diamond lattice, its existence is precluded if the crystal inversion symmetry is broken and the symmetry group of the crystal is reduced to the tetrahedral group T_d , which is the case for materials with a zinc-blende crystal structure. Using the paradigmatic example of the series of

cubic mercury chalcogenides HgX ($X = \text{Te}, \text{Se}, \text{S}$), we show that, indeed, even an infinitesimally small broken inversion symmetry (BIS) is detrimental for the existence of topological surface states. This sets helical semimetals apart from Weyl semimetals [22,23] in which a pair of Weyl points separated in momentum space results from the splitting of a 3D Dirac point due to either inversion or time-reversal symmetry breaking [24]. We show furthermore that, as expected, in the fully gapped TI regime, a BIS does not endanger the existence of topological surface states. In this case, the BIS rather renormalizes the Fermi velocity of the surface Dirac fermions in an anisotropic manner, similarly to the effect envisioned in anisotropic graphene superlattices [25,26]. This, in principle, allows an externally applied biaxial stress field to flip the surface-state chirality in a material with BIS.

HgX compounds. Pristine HgTe is a semimetal which is charge neutral when the Fermi energy is at the touching point between the light-hole (LH) and the heavy-hole (HH) Γ_8 bands at the BZ center [21,27]. The topological nature of the electronic states in this material cannot be inferred from these $p_{3/2}$ atomic levels, but rather follows from the inverted band ordering at the zone center of the LH Γ_8 band, which is particlelike, and the Γ_6 s band, which is holelike. In normal semiconductors, such as CdTe (see Fig. 1), Γ_6 forms the conduction band and Γ_8 is one of the valence bands. The consequence of this band inversion can be understood from the simple criterion derived by Fu and Kane [6] to distinguish normal and nontrivial topological classes. This criterion, strictly valid in the presence of inversion symmetry, establishes a material to be topologically nontrivial if two bands of opposite parity have level crossed with respect to the normal band ordering. The zinc-blende crystal structures of HgTe lack inversion symmetry, but it is normally considered that the BIS acts as a small perturbation and, invoking adiabatic continuity, does not hinder the topological nature of the level crossing. As the HH bands do not participate in the topological level crossing, it can be assumed that they act as inserted “parasitic” bulk bands, closing the full band gap and preventing the system from being a strong 3D TI. It is expected [20,21] that the existence of topological surface states resulting from

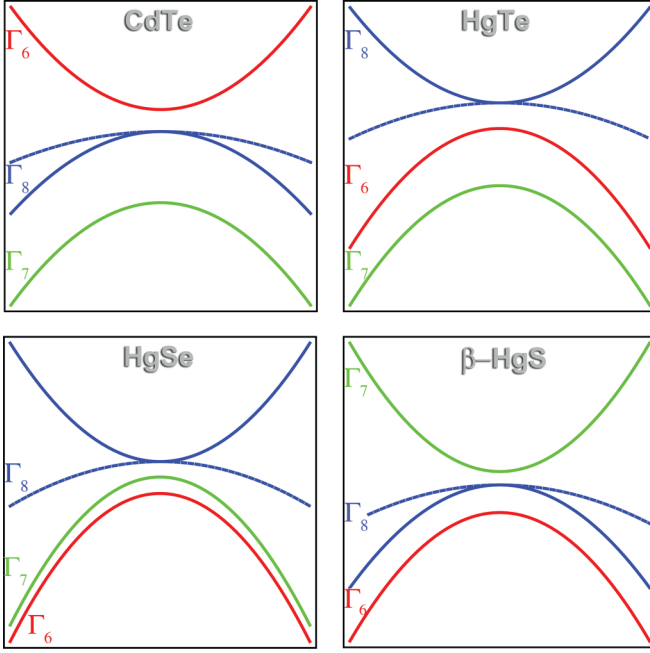


FIG. 1. (Color online) Schematic low-energy band structure of the HgX inverted semiconductors compared to the normal CdTe semiconductor.

the LH- Γ_6 TI bulk is not undermined by the presence of the HH bulk bands, suggesting that HgTe is a helical semimetal.

Similar arguments apply to HgSe, which has the same band ordering as HgTe but with the difference that the spin-orbit (SO) split-off Γ_7 bands are above the Γ_6 bands [28]: the SO splitting $\Delta_0 = E(\Gamma_8) - E(\Gamma_7)$ is smaller than the gap $-E_0 = E(\Gamma_8) - E(\Gamma_6)$ (cf. Fig. 1). In this case, the SO split-off bands, the LH bands, and the Γ_6 bands realize a bulk TI, with the HH bands playing, as in HgTe, the role of parasitic bands which close the full band gap. Yet another material of the same family—metacinnabar—was proposed to be topologically nontrivial: a recent fully relativistic electronic structure calculation [29] finds the required band ordering, although in this particular case the Γ_7 and Γ_6 bands have switched places with respect to the normal ordering (cf. Fig. 1) and thus $\Delta_0 < 0$. This reversed order is sufficient enough to create a small gap, thus rendering β -HgS a stoichiometric strong 3D TI.

Inversion invariant effective Hamiltonian. For an analysis of the topological surface states, one can rely on effective low-energy theories that are based upon a $\mathbf{k} \cdot \mathbf{p}$ expansion of the lowest energy bands around the Γ point. Within this approach, the quantum spin Hall effect in HgTe/CdTe quantum wells [3] has been correctly predicted. The generic form of a low-energy $\mathbf{k} \cdot \mathbf{p}$ expansion at the BZ center Γ for semiconductors with a zinc-blende crystal structure is given by the Kane model Hamiltonian [30]. Previous work has focused predominantly on the bands responsible for the level crossing, i.e., the Γ_6 and Γ_8 bands [21,27]. While such an analysis is capable of correctly describing the topological characteristics of HgTe, here we consider the full eight-band Kane model Hamiltonian, which takes into account the Γ_6 , Γ_7 , and Γ_8 bands and correctly describes the band ordering near the Brillouin-zone center of

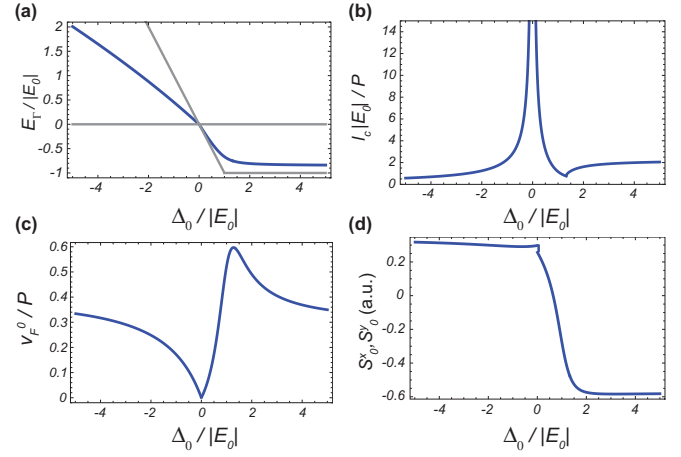


FIG. 2. (Color online) (a) Behavior of the energy of the surface Dirac point as a function of $\Delta_0/|E_0|$ neglecting BIS. The thin lines correspond to the conduction and valence bulk band edges by artificially removing the parasitic HH bands. (b)–(d) Behavior of the decay length of the surface states l_s , Fermi velocity of the surface Dirac cones v_F^0 , and the spin constants $S_0^{x,y}$ as a function of the spin-splitting energy Δ_0 .

the series of mercury chalcogenides HgX once the spin-orbit splitting energy Δ_0 is varied. This allows us to smoothly connect from the intrinsic, fully gapped, TI regime realized in β -HgS to the putative helical semimetal regime for $\Delta_0 > 0$ and analyze the fate of the resulting topological surface states. Even more Δ_0 not only provides a convenient tuning parameter, but its variation represents the physical effect of biaxial strain fields. Simultaneous application of two stress fields directed along the [100] ([010]) and [001] directions will, under specific conditions (see Supplemental Material [31]), preserve the degeneracy at the Γ point among the LH and HH bands, but renormalize the SO energy Δ_0 .

To establish the helical semimetal state in the cubic mercury chalcogenides assuming inversion symmetry is preserved, we explicitly calculate the [001] surface states of the eight-band Kane model Hamiltonian by neglecting BIS effects on the half space $z > 0$ [32] with open boundary conditions. For illustration of the physics, we take for simplicity the HgTe band structure parameters at $T = 0$ K [33]. At the Γ point of the surface BZ, the Kane model Hamiltonian predicts that the HH bands are completely decoupled from the other bands. The remaining part of the Hamiltonian is block diagonal with the two blocks for the chalcogen p -type (mercury s -type) states of total angular momentum $J_z = 1/2$ and $J_z = -1/2$, respectively. The eigenstates have therefore the form $\Psi^\uparrow(z) = (\psi_0^\uparrow, \mathbf{0})^T$ and $\Psi^\downarrow(z) = (\mathbf{0}, \psi_0^\downarrow)^T$, where $\psi_0^{\uparrow,\downarrow}$ is a three-dimensional spinor and $\mathbf{0}$ is a five-component zero vector. For the surface states, the wave function $\psi_0^{\uparrow,\downarrow}(z)$ is localized at the [001] surface, in which case $\Psi^{\uparrow,\downarrow}$ play the role of a spin-1/2 surface Kramer's doublet (see Supplemental Material [31]).

Figure 2(a) shows the energy of the surface Kramer's doublet as a function of the ratio among the SO splitting energy Δ_0 and the $\Gamma_6 - \Gamma_8$ gap, $-E_0$. In the intrinsic, fully gapped, TI regime ($\Delta_0 < 0$), the surface state's energy resides in the

direct bulk insulating gap at the Γ point. In the $\Delta_0 > 0$ regime, instead, the surface Kramer's doublet energy lies below the zero-energy HH band edge, but resides in the band gap of the TI bulk realized by the $\Gamma_{6,7}$ -LH bands. Figure 2(b) shows the behavior of the decay length of the surface states. We find that precisely at $\Delta_0 \equiv 0$ —where the gap of the bulk TI closes—the decay length diverges and thus the condition for the existence of the surface states is violated. For finite values of the spin-orbit splitting, instead, a renormalizable surface-state solution exists in the half-infinite space $z > 0$. By projecting the bulk Hamiltonian onto the subspace of these two surface states [9], we obtain an effective surface Hamiltonian to the leading order of $k_{x,y}$,

$$\mathcal{H}_{\text{surf}}(k_x, k_y) = E_{\Gamma} \mathcal{I} + v_F^0 (\sigma_x k_y - \sigma_y k_x), \quad (1)$$

where \mathcal{I} is the 2×2 identity matrix and v_F^0 is the Fermi velocity, the behavior of which as a function of the spin-orbit splitting is shown in Fig. 2(c). That the σ matrices in the effective surface model Hamiltonian are proportional to the real spin can be shown by projecting the total angular momentum operators $J_{x,y,z}$ onto the surface-state subspace. Independent of the spin-orbit splitting energy, we do find that $\langle \Psi | J_{x,y,z} | \Psi \rangle \equiv S_0^{x,y,z} \sigma_{x,y,z}$ where $S_0^z \equiv 1/2$, whereas $S_0^x \equiv S_0^y$ with a finite value whose behavior as a function of Δ_0 is shown in Fig. 2(d). As a result, the surface states show a linear dispersion with helical spin textures that are left handed for the surface conduction band and right handed for the surface valence band, proving the spin-momentum locking of the surface-state solutions. We emphasize that although in the semimetallic regime $\Delta_0 > 0$, the Dirac point is buried within the HH valence band, the existence of the surface Kramer's doublet is protected by point-group symmetries. Indeed, at the Γ point of the surface BZ, the total angular momentum J_z is still a good quantum number [3]. As argued in Ref. [3], any mixing among the HH bulk states with $J_z = \pm 3/2$ and the states with $J_z = \pm 1/2$ is prevented provided the axial symmetry around the \hat{z} axis and inversion symmetry are not broken. Away from the Γ point of the surface BZ, external perturbations due, for instance, to surface decorations can mix the HH bulk state with the topological surface states and lead to renormalizations of the surface state's dispersion [34].

Broken inversion symmetry. Having established that in the presence of inversion symmetry, the series of cubic mercury chalcogenides will either be in the strong 3D TI or in the helical semimetal state, we now take into account the intrinsic BIS of the zinc-blende crystal structure. From a $\mathbf{k} \cdot \mathbf{p}$ perspective, the BIS allows for additional terms in the bulk Hamiltonian once the point-group symmetry is reduced to T_d [27,30]. In the Kane model Hamiltonian (see Supplemental Material [31]), the BIS, indeed, yields additional linear-in- \mathbf{k} terms that stem from bilinear couplings consisting of $\mathbf{k} \cdot \mathbf{p}$ and SO interaction with the uppermost d core levels [35,36]. As a result, the parameter c is an elementary parameter of the Kane model [30]. Because of the smallness of the elementary parameter $c \simeq 80$ meV Å [36], the conventional wisdom [33] is that the BIS effect is very small in mercury chalcogenides and therefore can be safely neglected.

We do find, however, that the BIS has drastic consequences on both the existence conditions and the dispersion of the

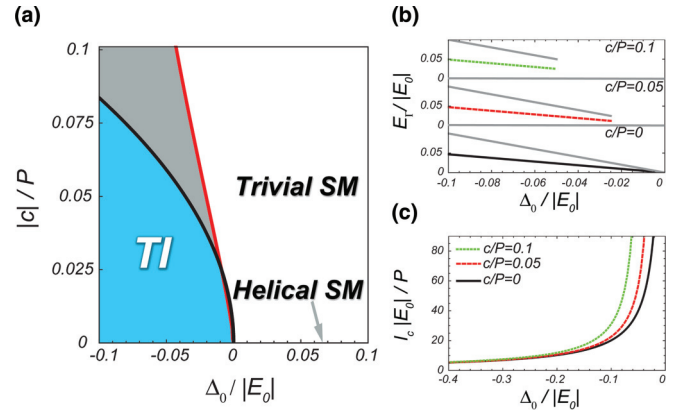


FIG. 3. (Color online) (a) Phase diagram for the existence of topological surface states at the [001] surface. The gray area corresponds to regions with topological surface states where the opening of the bulk band gap goes beyond the Kane model. (b) Behavior of the energy of the surface Dirac point as a function of $\Delta_0/|E_0|$ for different strengths of the BIS terms. The thin lines indicate the $\Gamma_{7,8}$ band edges at the Γ point of the BZ. (c) Same for the decay length of the surface states.

surface states. Independent of the actual c value, indeed, the BIS-induced linear-in- \mathbf{k} terms couple the HH with the TI bulk at the Γ point of the surface BZ. As a result, the BIS leads to an effective hybridization among the topological surface states and the parasitic HH bands. One would then expect that whenever the topological surface states overlap both in momentum and energy with the parasitic HH bands, they should be pushed away [18]. And, indeed, we find that for positive values of the spin-orbit splitting Δ_0 , in which case the energy of the surface Kramer's doublet lies below the zero-energy HH band edge, localized surface-state wave functions $\Psi^{\uparrow,\downarrow}$ at the BZ center *do not* exist. In the $\Delta_0 < 0$ regime instead, the BIS-induced hybridization should not be effective at the Γ point—the existence of the surface Kramer's doublet should not be hampered independent of the actual values of the c parameter and the spin-orbit splitting in this case. On the contrary, we find that the existence of topological surface states is intrinsically related to the strength of the linear-in- \mathbf{k} BIS terms and leads to the phase diagram shown in Fig. 3(a). Remarkably, for small values of the BIS parameter c , renormalizable surface states appear only whenever the spin-orbit splitting is negative by an amount sufficient to create a full indirect band gap. Thus, even in the absence of an overlap in momentum and energy with the parasitic HH bands, the topological surface states are prevented in the absence of a full bulk band gap, proving that the helical semimetal state is completely suppressed by the breaking of the O_h point group down to T_d .

Figure 3(b) shows the behavior of the surface Kramer's doublet energy at the surface BZ center for different values of the BIS parameter c when the intrinsic, fully gapped, TI regime is reached. It always lies in the bulk gap at the zone center among the Γ_8 and the SO split-off Γ_7 bands. We also show [cf. Fig. 3(c)] the behavior of the penetration depth of the surface states which, increasing the value of the spin-orbit splitting Δ_0 , increases and eventually diverges at the critical

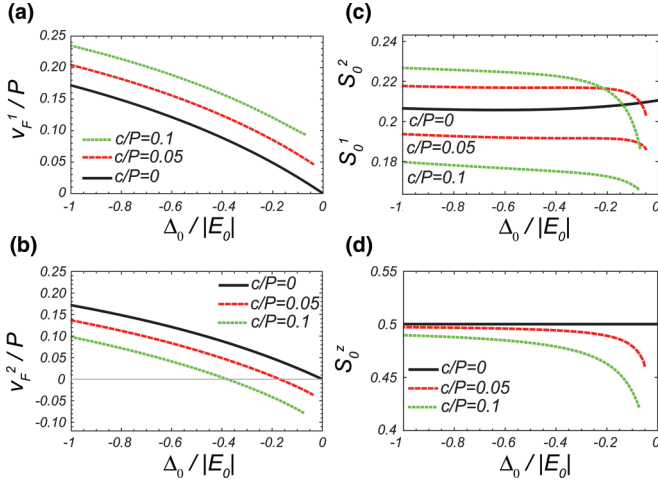


FIG. 4. (Color online) (a),(b) Behavior of the two nonequivalent Fermi velocities of the surface Dirac cones vs $\Delta_0/|E_0|$ for different values of the c parameter. (c),(d) Same for the spin constants $S_0^{1,2,z}$.

line of the phase diagram in Fig. 3(a). We find that in the presence of BIS terms, the effective surface Hamiltonian to the leading order of $k_{x,y}$ reads

$$\mathcal{H}_{\text{surf}}(k_x, k_y) = E_\Gamma \mathcal{I} + v_F^1 k_1 \sigma_1 - v_F^2 k_2 \sigma_2, \quad (2)$$

where $k_{1,2} = (k_x \pm k_y)/\sqrt{2}$ and $\sigma_{1,2}$ are the corresponding rotated Pauli matrices $\sigma_{1,2} = (\sigma_x \mp \sigma_y)/\sqrt{2}$. As a result, the surface Dirac cones are anisotropic ($v_F^1 \neq v_F^2$) along the diagonal directions of the surface BZ, as can be shown by a two-dimensional $\mathbf{k} \cdot \mathbf{p}$ analysis (see Supplemental Material [31]) and in perfect agreement with the density functional electronic structure calculations in β -HgS [29]. In addition, the spin-momentum locking of the surface states is guaranteed

by the fact that by projecting the $\pi/4$ rotated total angular momentum operators $J_{1,2,z}$ onto the subspace of the surface states at the BZ center, we find $\langle \Psi | J_{1,2,z} | \Psi \rangle \equiv S_0^{1,2,z} \sigma_{1,2,z}$ with $S_0^{1,2,z}$ some constants, the behavior of which, as a function of Δ_0 , is shown in Figs. 4(c) and 4(d). Figures 4(a) and 4(b) show the behavior of the two inequivalent Fermi velocities for different values of the BIS parameter c . For $\Delta_0 \ll E_0$, the surface Dirac cone is strongly anisotropic with a large dispersion along the diagonal k_1 and a nearly flat behavior along the perpendicular direction. By varying the spin-orbit splitting energy, we find a critical value Δ_0^c where the degree of anisotropy v_F^1/v_F^2 diverges. The fact that only one of the two nonequivalent Fermi velocities changes sign at this value implies a change in the handedness of the surface Dirac cone—left handed for $\Delta_0 < \Delta_0^c$ and right handed for $\Delta_0 > \Delta_0^c$ in the surface conduction band. Therefore, a suitable application of anisotropic biaxial stresses can induce a flip of chirality, which would immediately manifest itself as a sign change of the quantized Hall conductance in the presence of time-reversal symmetry-breaking surface perturbations.

Conclusions. The coexistence of bulk metallic states with topological surface states can be encountered in a large class of materials. Inverted zero-gap semiconductors fall into this class and provide a prominent example of a helical semimetal. We have shown here that while such a state of matter can be established in the presence of full cubic symmetry, the absence of bulk inversion symmetry allows for a coupling of bulk and surface states, leading to a loss of the surface states as proper surface bound states. As a consequence, the helical semimetallic state ceases to exist. In the intrinsic, fully gapped, TI regime, the broken inversion symmetry strongly renormalizes the anisotropy of the group velocity of the surface Dirac fermions, similarly to graphene superlattices [25,26].

Acknowledgment. The authors thank M. Richter and F. Viot for very fruitful discussions.

-
- [1] C. L. Kane and E. J. Mele, *Phys. Rev. Lett.* **95**, 226801 (2005).
 [2] C. L. Kane and E. J. Mele, *Phys. Rev. Lett.* **95**, 146802 (2005).
 [3] B. A. Bernevig, T. L. Hughes, and S.-C. Zhang, *Science* **314**, 1757 (2006).
 [4] C. Wu, B. A. Bernevig, and S.-C. Zhang, *Phys. Rev. Lett.* **96**, 106401 (2006).
 [5] M. König, S. Wiedmann, C. Brüne, A. Roth, H. Buhmann, L. W. Molenkamp, X.-L. Qi, and S.-C. Zhang, *Science* **318**, 766 (2007).
 [6] L. Fu and C. L. Kane, *Phys. Rev. B* **76**, 045302 (2007).
 [7] L. Fu, C. L. Kane, and E. J. Mele, *Phys. Rev. Lett.* **98**, 106803 (2007).
 [8] J. E. Moore and L. Balents, *Phys. Rev. B* **75**, 121306 (2007).
 [9] H. Zhang, C.-X. Liu, X.-L. Qi, X. Dai, Z. Fang, and S.-C. Zhang, *Nat. Phys.* **5**, 438 (2009).
 [10] D. Hsieh, D. Qian, L. Wray, Y. Xia, Y. S. Hor, R. J. Cava, and M. Z. Hasan, *Nature (London)* **452**, 970 (2008).
 [11] Y. Xia, D. Qian, D. Hsieh, L. Wray, A. Pal, H. Lin, A. Bansil, D. Grauer, Y. S. Hor, R. J. Cava, and M. Z. Hasan, *Nat. Phys.* **5**, 398 (2009).
 [12] Y. L. Chen, J. G. Analytis, J.-H. Chu, Z. K. Liu, S.-K. Mo, X. L. Qi, H. J. Zhang, D. H. Lu, X. Dai, Z. Fang, S. C. Zhang, I. R. Fisher, Z. Hussain, and Z.-X. Shen, *Science* **325**, 178 (2009).
 [13] D. Hsieh, Y. Xia, L. Wray, D. Qian, A. Pal, J. H. Dil, J. Osterwalder, F. Meier, G. Bihlmayer, C. L. Kane, Y. S. Hor, R. J. Cava, and M. Z. Hasan, *Science* **323**, 919 (2009).
 [14] M. Z. Hasan and C. L. Kane, *Rev. Mod. Phys.* **82**, 3045 (2010).
 [15] B. Rasche, A. Isaeva, M. Ruck, S. Borisenko, V. Zabolotnyy, B. Büchner, K. Koepf, C. Ortix, M. Richter, and J. van den Brink, *Nat. Mater.* **12**, 422 (2013).
 [16] A. R. Akhmerov, J. Nilsson, and C. W. J. Beenakker, *Phys. Rev. Lett.* **102**, 216404 (2009).
 [17] K. Eto, Z. Ren, A. A. Taskin, K. Segawa, and Y. Ando, *Phys. Rev. B* **81**, 195309 (2010).
 [18] D. L. Bergman and G. Refael, *Phys. Rev. B* **82**, 195417 (2010).
 [19] D. L. Bergman, *Phys. Rev. Lett.* **107**, 176801 (2011).
 [20] C. Brüne, C. X. Liu, E. G. Novik, E. M. Hankiewicz, H. Buhmann, Y. L. Chen, X. L. Qi, Z. X. Shen, S. C. Zhang, and L. W. Molenkamp, *Phys. Rev. Lett.* **106**, 126803 (2011).

- [21] R.-L. Chu, W.-Y. Shan, J. Lu, and S.-Q. Shen, *Phys. Rev. B* **83**, 075110 (2011).
- [22] X. Wan, A. M. Turner, A. Vishwanath, and S. Y. Savrasov, *Phys. Rev. B* **83**, 205101 (2011).
- [23] L. Balents, *Physics* **4**, 36 (2011).
- [24] S. M. Young, S. Zaheer, J. C. Y. Teo, C. L. Kane, E. J. Mele, and A. M. Rappe, *Phys. Rev. Lett.* **108**, 140405 (2012).
- [25] C.-H. Park, L. Yang, Y.-W. Son, M. L. Cohen, and S. G. Louie, *Nat. Phys.* **4**, 213 (2008).
- [26] C.-H. Park, Y.-W. Son, L. Yang, M. L. Cohen, and S. G. Louie, *Nano Lett.* **8**, 2920 (2008).
- [27] X. Dai, T. L. Hughes, X.-L. Qi, Z. Fang, and S.-C. Zhang, *Phys. Rev. B* **77**, 125319 (2008).
- [28] A. Svane, N. E. Christensen, M. Cardona, A. N. Chantis, M. van Schilfgaarde, and T. Kotani, *Phys. Rev. B* **84**, 205205 (2011).
- [29] F. Virost, R. Hayn, M. Richter, and J. van den Brink, *Phys. Rev. Lett.* **106**, 236806 (2011).
- [30] R. Winkler, *Spin-Orbit Coupling Effects in Two-Dimensional Electron and Hole Systems* (Springer, Berlin, 2003).
- [31] See Supplemental Material at <http://link.aps.org/supplemental/10.1103/PhysRevB.89.121408> for detailed information about the Kane model Hamiltonian, the corresponding surface-state solutions, and a two-dimensional $\mathbf{k} \cdot \mathbf{p}$ theory of the surface band structure.
- [32] C.-X. Liu, X.-L. Qi, H.-J. Zhang, X. Dai, Z. Fang, and S.-C. Zhang, *Phys. Rev. B* **82**, 045122 (2010).
- [33] E. G. Novik, A. Pfeuffer-Jeschke, T. Jungwirth, V. Latussek, C. R. Becker, G. Landwehr, H. Buhmann, and L. W. Molenkamp, *Phys. Rev. B* **72**, 035321 (2005).
- [34] F. Virost, R. Hayn, M. Richter, and J. van den Brink, *Phys. Rev. Lett.* **111**, 146803 (2013).
- [35] G. Dresselhaus, *Phys. Rev.* **100**, 580 (1955).
- [36] M. Cardona, N. E. Christensen, and G. Fasol, *Phys. Rev. Lett.* **56**, 2831 (1986).